# Anomalous Bending of a Polyelectrolyte

Roya Zandi
*Department of Chemistry and Biochemistry, UCLA, Box 951569, Los Angeles, California, 90095-1569*

Joseph Rudnick
*Department of Physics and Astronomy, UCLA, Box 951547, Los Angeles, CA 90095-1547*

Ramin Golestanian
*Institute for Advanced Studies in Basic Sciences, Zanjan 45195-159, Iran*
*Institute for Studies in Theoretical Physics and Mathematics, P.O. Box 19395-5531, Tehran, Iran*
*Laboratoire de Physique de la Matière Condensée, Collège de France, UMR 7125 et FR 2438 du CNRS, 11 place Marcelin-Berthelot, 75231 Paris Cedex 05, France*

(Dated: February 1, 2008)

We report on a study of the shape of a stiff, charged rod that is subjected to equal and opposite force couples at its two ends. Unlike a neutral elastic rod, which forms a constant curvature configuration under such influences, the charged rod tends to flatten in the interior and accumulate the curvature in the end points, to maximally reduce the electrostatic self-repulsion. The effect of this nonuniform bending on the effective elasticity and on the statistical conformations of a fluctuating charged rod is discussed. An alternative definition for the electrostatic persistence length is suggested. This new definition is found to be consistent with a corresponding length that can be deduced from the end-to-end distribution function of a fluctuating polyelectrolyte.

PACS numbers: 82.35.Rs, 87.15.La, 36.20.-r, 82.35.Lr

## I. INTRODUCTION AND SUMMARY

Given the ubiquity of charged linear structures in biology, and their fundamental importance to essential processes in living systems, the relationship of Coulomb interactions to the mechanical properties of polyelectrolytes is a topic of pressing interest. Indeed, there have been a number of theoretical [1, 2, 3, 4, 5, 6] and experimental [7, 8, 9] studies of the behavior of charged polymeric chains, with an eye to elucidating the various influences that control their equilibrium and statistical characteristics. In spite of the considerable effort expended, there is, as yet, no comprehensive theoretical description of the way in which charged chains respond to environmental influences.

The basic theoretical model of a polyelectrolyte chain (PE) is simplicity itself. A rod with an intrinsic elasticity quantified in terms of a bending modulus carries charges, either uniformly distributed along it, or concentrated at points along its axis. The energy of this chain consists entirely of the elastic energy associated with bending of the rod and the electrostatic energy of interaction of the charges on the rod. The electrostatic interaction may be screened by counterions in solution in the vicinity of the rod. This screening is assumed to be Debye-like.

The characterization of the effects of intrinsic stiffness of a neutral inextensible, or worm-like, chain (WLC) in terms of a *persistence length* is by now well-established [10]. This quantity describes the exponential decay of correlations in the orientation of the backbone of a WLC. It is directly related to the energy stored in a short segment of the WLC which has been bent as the result of the application of force couples at its end points. An extension of the persistence length to the case of a PE, due to Odijk [11] utilizes this basic approach to obtain that quantity in the case of a stiff, charged rod. In calculating the energy of the bent segment of the PE, Odijk assumed that the shape of this segment is not affected by the Coulomb interactions, an assumption shared by all other expressions for the effective persistence length of a PE of which we are currently aware [12, 13, 14]. This leads to a remarkably successful analytic expression for the persistence length [see Eq. (6) in the next section]. This approximation does not work in all regimes; in previous work, we have identified the regimes in which this assumption is correct and other regimes in which it fails to give rise to accurate answers [15, 16].

The general question of the applicability of the notion of a persistence length to a PE in the rod-like limit was explored in the above mentioned work [15, 16] by the current authors. This study was conducted in the context of a calculation of the thermal distribution of end-to-end distances of an ensemble of rod-like PE's. It was found that there are regimes in which this distribution differs substantially from the corresponding distribution for neutral WLC's. When this is the case, the effective persistence length associated with the end-to-end distance distribution (or radial distribution) is not consistent with the formula derived in Ref. [11]. The effective persistence length is obtained in reference [15, 16] by matching the PE distribution as closely as possible to the radial distribution of uncharged worm-like chains

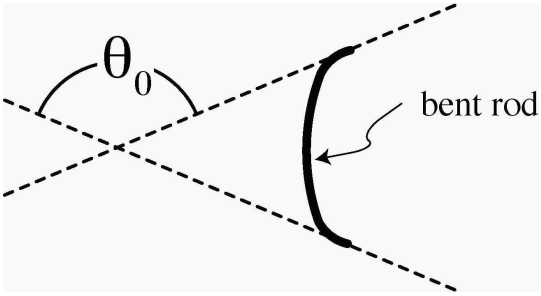


FIG. 1: The bent rod. The angle $\theta_0$ between the two ends is illustrated. The relationship between the angle $\theta_0$ and the energy, $\mathcal{E}$, stored the bent rod is displayed in Eq. (1.

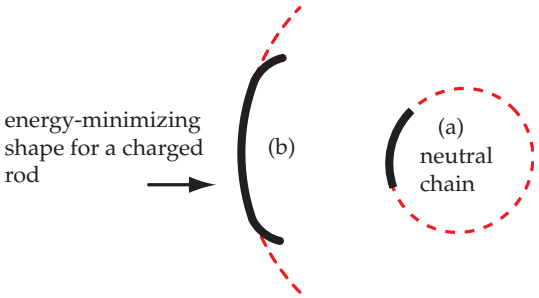


FIG. 2: The energy-minimizing shape of a charged rod with full treatment of electrostatic interactions and end effects (plot (a)). Plot (b) corresponds to the energy-minimizing shape of a WLC. A segment of a neutral WLC forms an arc of a circle while the curvature of a PE segment can be concentrated at its ends.

[17].

In this paper, we undertake a calculation of the effective persistence length. Our approach is identical in overall philosophy to the that utilized by Odijk [11]. A rod is subjected to external torques that causes it to bend. The energy, $\mathcal{E}$, in the bent rod is calculated and related to, $\theta_0$, the difference in angles at the two ends, as shown in Fig. 1. The precise relationship between the energy, $\mathcal{E}$, in the rod and the angle $\theta_0$ is

$$\frac{\mathcal{E}}{k_{\rm B}T} = \frac{\theta_0^2}{2}\frac{\ell_p}{L}. \qquad (1)$$

Here, $L$ is the total length of the rod. In Odijk's approach, it is assumed that the bent rod takes the form of an arc of a circle. This is true if all of the energy is elastic. However, in the case of interest here, a significant portion of the energy may be electrostatic in nature. The fundamental improvement over Odijk's calculational method is that we determine the actual shape of the bent rod, taking into account the effects of screened and unscreened electrostatic interactions. We assume that the shape taken is controlled by the requirement that, in the absence of thermal fluctuations, the rod minimizes its total energy. The expression obtained for the rod's shape is directly related to the inverse of the Hamiltonian that relates the energy of the bent rod to its distortion from a straight line. This approach leads to new results for the shape of the rod and to alterations in the energy and the persistence length as defined in Eq. (1).

We find that there are, in certain regimes, dramatic differences between the shape of a short PE under the influence of force couples at its ends and the shape of a similarly torqued WLC. In such regimes the curvature of a PE is concentrated at its ends, while the WLC distorts into a circular arc, as illustrated in Fig. 2. In regimes in which the shapes of the PE and WLC coincide, we find that the Odijk's formula for the effective persistence length is accurate. However, when the shape of the bent PE is inconsistent with the assumption of constant curvature, the electrostatic persistence length derived from Eq. (1) deviates from Odijk's result. On the other hand, this persistence length is compatible with the persistence length deduced from the statistics of the conformations of a fluctuating PE described by the radial distribution function [15, 16].

The rest of the paper is organized as follows. Section II introduces the basic elastic model for PE's, followed by a general description on how one obtains the equilibrium shape of a PE in Sec. III. The results for the shape of a PE are presented in Sec. IV, and it is shown in Sec. V how a persistence length can be deduced from the PE profile. The suggested electrostatic persistence length is then compared with Odijk's formula and also the persistence length that one can extract from the radial distribution of the PE in Sec. VI, which is then followed by concluding remarks in Sec. VII. Some details of the calculations are relegated to appendices.

## II. MODEL ELASTICITY FOR POLYELECTROLYTES

As noted above, we treat the polyelectrolyte as an inextensible charged rod. The total energy of such a rod is the sum of the intrinsic elasticity and the screened electrostatic interaction energy. We assume that the electrostatic interaction is screened by counterions that adjust more or less instantaneously to changes in the overall shape of the polyelectrolyte. Because of the inextensibility of the PE's under consideration [11, 17], we adopt Kratky and Porod WLC model to describe the bending energy of the chain [18]. In this model, polymers are represented by a space curve $\mathbf{r}(s)$ as a function of the arc length parameter $s$. The total energy of the chain is given by

$$\frac{\mathcal{E}}{k_{\rm B}T} = \frac{\ell_{p0}}{2}\int_0^L ds\left(\frac{d\mathbf{t}(s)}{ds}\right)^2 + \frac{\beta}{2}\int_0^L dsds'\frac{e^{-\kappa|\mathbf{r}(s)-\mathbf{r}(s')|}}{|\mathbf{r}(s)-\mathbf{r}(s')|}, \qquad (2)$$

where $\mathbf{t}$ is the unit tangent vector. The second term in the Eq. (2) is the Debye-Hückel potential, in which screening is controlled by the Debye length $\kappa^{-1}$ that is a measure of the ionic strength of the solvent. The quantity $\beta = \ell_{\rm B}/b^2$ is the strength of the electrostatic interac-

tion with $b$ the average separation between neighboring charges and $\ell_{\rm B} = e^2/\epsilon k_B T$ the Bjerrum length. The quantity $\epsilon$ is the dielectric constant of the ion-free solvent.

The chain is assumed to be sufficiently stiff that excluded volume does not play a role. We will consider PE's whose length, $L$, is either comparable with or long compared to the intrinsic persistence length, $\ell_{p0}$. In both cases, we restrict our consideration to regions in which the combination of intrinsic stiffness and repulsive strength of the Coulomb interaction keeps the chains in their rodlike limit [19]. We do not take into account the fluctuation in the charges localized to the chain and in the counterion system that can give rise to attractive interactions leading to chain collapse [20, 21].

Orienting the tangent vector at one end of the PE, $\mathbf{t}(0)$, so that it points in the positive $\mathbf{z}$ direction, we characterize $\mathbf{t}(s)$ by two angles of rotation: $\theta_x(s) = \arctan[t_x(s)/\sqrt{1-t_x^2(s)-t_y^2(s)}]$ in the $xz$ plane and $\theta_y(s) = \arctan[t_y(s)/\sqrt{1-t_x^2(s)-t_y^2(s)}]$ in the $yz$ plane. For polyelectrolytes in the rodlike limit, $\theta_x(s)$ and $\theta_y(s)$ are small. With the help of the relation $\mathbf{r}(s) - \mathbf{r}(s') = \int_s^{s'} du\, \mathbf{t}(u)$, we are able to expand both the bending energy and the screened Coulomb interaction about the rodlike configuration up to quadratic order in $\vec{\theta}(s) = (\theta_x(s), \theta_y(s))$ following the Ref. [10, 11]. In this case, Eq. (2) can be written:

$$\begin{aligned}\frac{\mathcal{E}}{k_{\rm B}T} &= \frac{\ell_{p0}}{2}\int_0^L ds\left\{\left(\frac{d\theta_x(s)}{ds}\right)^2+\left(\frac{d\theta_y(s)}{ds}\right)^2\right\}\\ &+\frac{\beta}{2}\int_0^L\int_0^L ds\; ds'\mathcal{L}\,(s,s')\\ &\times\;\{\theta_x(s)\theta_x(s')+\theta_y(s)\theta_y(s')\}\,, \end{aligned} \tag{3}$$

where the electrostatic kernel is given by

$$\begin{aligned}&\mathcal{L}(s,s') = \int_0^L ds_1 ds_2 \frac{[1+\kappa(s_2-s_1)]\mathrm{e}^{-\kappa(s_2-s_1)}}{(s_2-s_1)^3}\\ &\times\{(s_2-s_1)\left[\Theta(s-s_1)-\Theta(s-s_2)\right]\delta(s-s')\\ &-\left[\Theta(s-s_1)-\Theta(s-s_2)\right]\left[\Theta(s'-s_1)-\Theta(s'-s_2)\right]\}\,,\end{aligned} \tag{4}$$

with $\Theta(s)$ the Heaviside step function.

Equations (3) and (4) constitute the expression for the energy utilized by Odijk in his calculation of the electrostatic persistence length. The essence of this calculation is to constrain the difference between the orientation of the tangent vectors at each end of the rod, $\theta(L) - \theta(0) \equiv \theta_0$ and then to determine the energy, $\mathcal{E}$ of the bent rod with the use of the formulas in Eqs. (3) and (4). The persistence length, $\ell_p$, is then given by Eq. (1). In his calculation of the total energy of a bent segment of PE, Odijk makes the approximation that the segment is characterized by a constant curvature [11]. That is, he assumes that the electrostatic interaction does not cause the shape of the PE to differ from that of a WLC segment. According to this picture, $\theta_{x,y}(s)$ are linear functions of $s$. One can then obtain an explicit, analytical expression for the total energy of a bent polyelectrolyte segment, which leads directly to the following prediction for the persistence length of such a charged rod through Eq. (1):

$$\ell_p = \ell_{p0} + \ell_{\rm Odijk}, \tag{5}$$

where

$$\begin{aligned}\ell_{\rm Odijk} &= \frac{\beta L^2}{12}\left[e^{-\kappa L}\left(\frac{1}{\kappa L}+\frac{5}{(\kappa L)^2}+\frac{8}{(\kappa L)^3}\right)\right.\\ &\left.+\frac{3}{(\kappa L)^2}-\frac{8}{(\kappa L)^3}\right].\end{aligned} \tag{6}$$

In the next section, we sketch a general method of calculating the equilibrium shape of elastic charged rods under the influence of applied bending forces. This leads to a prescription for the calculation of persistence length based on the energy of the bent PE.

## III. THE GENERAL STRATEGY FOR FINDING THE ENERGY-MINIMIZING SHAPE OF A BENT POLYELECTROLYTE

As noted previously, the principal advance in our approach to the bending energy of a PE is that we calculate the actual shape of the bent rod. Here, we discuss the general approach to this calculation. The energy of the rod in Eq. (3) can be expressed as the expectation value of the energy operator,$\mathcal{H}$, i.e.

$$\frac{\mathcal{E}}{k_{\rm B}T} = \frac{1}{2}\int_0^L\int_0^L ds ds'\;\theta(s)\mathcal{H}(s,s')\theta(s'). \tag{7}$$

where $\mathcal{H}$, the bilinear "energy" operator, is equal to

$$\mathcal{H} = -\ell_{p0}\frac{d^2}{ds^2}\delta(s-s') + \beta\mathcal{L}(s,s'). \tag{8}$$

To obtain the response of a polyelectrolyte to force couples at its two ends, we minimize the energy expression in Eq. (7) with respect to $\theta_{x,y}(s)$, subject to the following boundary conditions:

$$\begin{aligned}\theta_x(0) &= 0,\\ \theta_y(0) &= 0,\\ \theta_x(L) &= \theta_{0x},\\ \theta_y(L) &= \theta_{0y},\end{aligned} \tag{9}$$

where the angles $\theta_{0x}$ and $\theta_{0y}$ are assumed to be very small, in order to keep the chain in the rod-like limit. The resulting Euler-Lagrange equations are completely

decoupled with respect to both variables $\theta_x(s)$ and $\theta_y(s)$; therefore, we focus on planar deformations which can be characterized entirely in terms of a single angle $\theta(s)$. In this case, the boundary conditions are simply,

$$\begin{aligned} \theta(0) &= 0, \\ \theta(L) &= \theta_0. \end{aligned} \tag{10}$$

We enforce these boundary conditions via Lagrange multipliers by adding the terms

$$-\int_0^L \{\lambda_0 \delta(s)\theta(s) - \lambda_L \delta(s-L)\theta(s)\}\, ds, \tag{11}$$

to the energy in Eq. (7). Then we seek the solution that minimizes the energy $\mathcal{E}$ in terms of an eigenfunction expansion of the form

$$\theta_{\min}(s) = \sum_{n=0}^{\infty} c_n \psi_n(s), \tag{12}$$

where $\psi_n(s)$ are eigenfunctions of the bilinear Euler-Lagrange "energy" operator $\mathcal{H}$ in Eq. (8).

The solution to the minimization equation, which is now in terms of the amplitudes $c_n$, is

$$c_j = \frac{\lambda_0 \psi_j(0) + \lambda_L \psi_j(L)}{\epsilon_j}, \tag{13}$$

where $\epsilon_j$'s are the eigenvalues of Eq. (8). The values of $\epsilon_j$'s depend on the three dimensionless parameters, $\beta L$, $\kappa L$, and $\ell_{p0}/L$. Rotational invariance implies that there must be one eigenfunction, $\psi_0(s) = 1/\sqrt{L}$, with eigenvalue $\epsilon_0 = 0$. This is due to the fact that simply tilting the rod, which yields a constant value for $\theta(s)$, does not change the energy. All other eigenfunctions possess positive eigenvalues. Equation (13) shows that there is a singularity at $\epsilon_0 = 0$. We can remove the singularity by adding a term of the form $\frac{g}{2}\theta(s)^2$ to the energy in Eq. (7). The parameter $g$ is a small "gap" parameter that will be set equal to zero at the end. The quantity $g$ is thus added to the denominator of Eq. (13), and there is no longer a singularity at $\epsilon_0 = 0$ unless $g = 0$.

We adjust the Lagrange multipliers, $\lambda_0$ and $\lambda_L$, using the boundary conditions of Eq. (10). The two equations that lead to the results for the $\lambda$'s are

$$\begin{aligned} \theta(0) &= \frac{1}{\sqrt{L}}\frac{\lambda_0+\lambda_L}{g} + \sum_{n=1}^{\infty} \psi_n(0)\frac{\lambda_0\psi_n(0)+\lambda_L\psi_n(L)}{\epsilon_n+g} \\ &= 0, \end{aligned} \tag{14}$$

$$\begin{aligned} \theta(L) &= \frac{1}{\sqrt{L}}\frac{\lambda_0+\lambda_L}{g} + \sum_{n=1}^{\infty} \psi_n(L)\frac{\lambda_0\psi_n(0)+\lambda_L\psi_n(L)}{\epsilon_n+g} \\ &= \theta_0. \end{aligned} \tag{15}$$

The above equations reveal that the only possible way in which we can obtain finite values for the angles at 0 and $L$ is to have $\lambda_L \to -\lambda_0$ as $g \to 0$. Let us set $\lambda_0 + \lambda_L = gA\sqrt{L}$, where $A$ is a constant that is set by adjusting boundary conditions. The general solution for $\theta(s)$ in the limit $g = 0$ is, then,

$$\theta(s) = A + \lambda_0 \sum_{n=1}^{\infty} \psi_n(s)\frac{\psi_n(0) - \psi_n(L)}{\epsilon_n}. \tag{16}$$

The limiting result of equal and opposite $\lambda$'s makes sense if we think of those Lagrange multipliers in terms of torques, or force couples, applied at the two ends of the PE segment. Given such a picture, we know that unless the two torques are equal and opposite, there will be an uncontrolled rotation of the segment. It is, in fact, possible to set up a calculation of the shape of a segment under the influence of such torques. Energy minimization yields equations for the angles at the ends of the segment that are precisely as given by Eqs. (14) and (15), with the $\lambda$'s proportional to the torques at each end.

In the next section we calculate numerically the energy-minimizing shape of a charged rod and compare it with an arc of circle. This will lead to greater insight into the influence of energetics on the classical shape of a bent segment of PE. It will also allow us to test the fundamental relevance of an energy calculation such as the one described above to the persistence length of a PE, defined in terms of its conformational statistics.

## IV. NONUNIFORM BENDING OF CHARGED ELASTIC RODS

The expression for $\theta$ given in Eq. (16) can also be written as

$$\theta(s) = A + \lambda_0(K(s,L) - K(s,0)), \tag{17}$$

where

$$K(s,s') = \sum_{n=1}^{\infty} \frac{\psi_n(s)\psi_n(s')}{\epsilon_n}, \tag{18}$$

It is readily demonstrated that the quantity $K(s,s')$ defined in (18) is the inverse of the energy operator in Eq. (8). The operator $K(s,s')$ has been calculated with the use of a cosine function basis set in Refs. [15, 16]. We utilize our previously-obtained results for the inverse operator to numerically calculate the quantity $\theta$ in Eq. (16). An outline of the construction of the energy in this basis set is contained in Appendix A.

In the absence of electrostatic interaction, a bent elastic rod conforms to an arc of a circle, which is described by a linear solution for Eq. (17). In Fig. 3, the energy-minimizing shapes of charged rods with $\kappa L = 10$, $\ell_{p0}/L = 0.5$, and different values of $\beta L$, are compared with that of a corresponding neutral chain. As the figure clearly illustrates, a $\theta(s)$ that depends linearly on arc length, $s$, does not correspond to the minimum energy configuration of bent charged elastic rods, which tend to

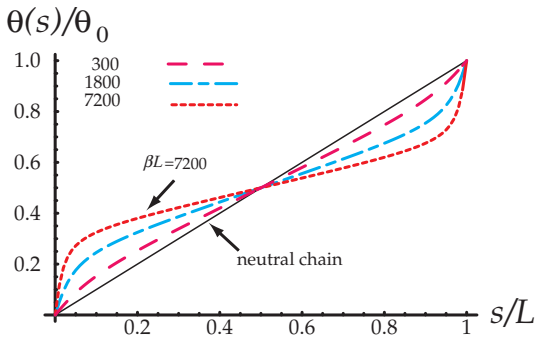


FIG. 3: Plots of the energy-minimizing shape for charged elastic rods [Eq. (16)] at $\kappa L = 10$, $\ell_{p0}/L = 0.5$ and $\beta L = 300$ (dashed line), $\beta L = 1800$ (dashed and dotted line), $\beta L = 7200$ (dotted line). The neutral chain forms an arc of a circle (represented by a straight line). As $\beta L$ increases, charged chains tends to flatten more in the interior and accumulate curvature in the end points. The extreme range of $\beta L$ is intended to clearly indicate the influence of charging on shape.

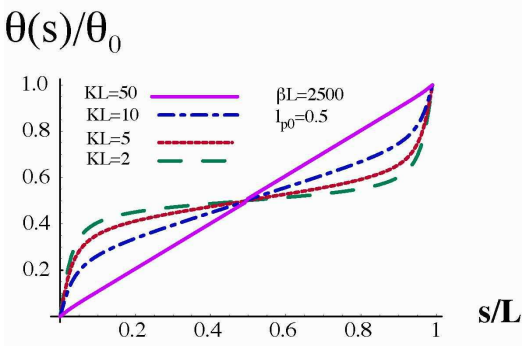


FIG. 4: Plot of $\theta(s)/\theta_0$ for a charged rod, corresponding to various values of the inverse screening length, $\kappa$. In all plots $\ell_{p0} = 50$ nm, $\beta = 25$ nm$^{-1}$ (corresponding to DNA) and $L = 100$ nm. The values of the screening parameters are $\kappa = 0.5$ nm$^{-1}$ (thick line), $\kappa = 0.1$ nm$^{-1}$ (dashed and dotted line), $\kappa = 0.05$ nm$^{-1}$ (dotted line), and $\kappa = 0.02$ nm$^{-1}$ (dashed line), respectively.

flatten in the interior and accumulate curvature in the exterior (see Fig. 2 above). This is in part because the electrostatic self-repulsion is lower in the end points due to the reduction in repelling neighboring charges there. Figure 3 also highlights the fact that deviations from constant curvature become more pronounced as the charging strength, $\beta L$ increase. This tendency reinforces the notion that Coulomb repulsion underlies the concentration of curvature near the ends of the bent rod.

We have also investigated the influence of inverse screening length, $\kappa$, and absolute length, $L$, on the shape of a bent PE segment. Figure 4 illustrates the effects of a change of $\kappa$ on the arclength dependence of $\theta$. In this figure, the bare persistence length $\ell_{p0} = 50$ nm and the charging parameter $\beta = 25$ nm$^{-1}$ corresponding to DNA are used, and the length of the segment is set equal to 100 nm. It is apparent that as the screening length increases the shape of the bent segment deviates more and more from an arc of a circle.

Additionally, we have looked at the consequences on PE shape of changes in the length of the segment, keeping all other parameters fixed. Figure 5 shows how changing the length, $L$, causes $\theta(s)$ to deviate from a straight line. As in Fig. 4, we have set $\ell_{p0}$ equal to 50 nm and $\beta$ equal to 25 nm$^{-1}$, as corresponding to DNA. The inverse screening length $\kappa$ in Fig. 5 is fixed at 0.1 nm$^{-1}$.

The nonlocal electrostatic interaction seems to favor a decomposition of the linear profile into a piece-wise linear one, in which the interior takes up a lower curvature and the two end-segments in the exterior acquire a higher curvature. The relatively sharp changes in the slope that result in "shoulders" in the profile take place symmetrically at positions denoted by $s_c$ and $L - s_c$, which can be defined in terms of the intersection points of the tangents to the various segments of the profile, as illustrated in Fig. 6.

The position of the shoulder $s_c$ is a monotonically de-

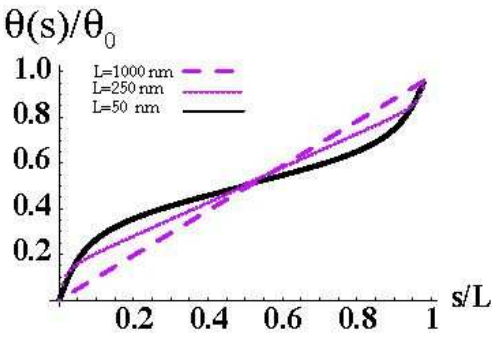


FIG. 5: Plot of $\theta(s)/\theta_0$ for a charged rod for which the length $L$ is allowed to vary. In all curves $\ell_{p0} = 50$ nm, $\beta = 25$ nm$^{-1}$ (corresponding to DNA) and $\kappa = 0.1$ nm$^{-1}$. It is evident that longer segments behave more like a WLC in that when bent they take a shape with a constant curvature. This reflects the influence on the shape of the combination $\kappa L$, and is consistent with the tendencies indicated in Fig. 4.

creasing function of $\beta L$ as shown in Fig. 7. The effect of $\ell_{p0}/L$ on the $s_c$ is also illustrated in Fig. 7. As seen in the figure, the shoulder $s_c$ increases upon increasing the intrinsic persistence length of the chain. The dependence of $s_c$ on screening, on the other hand, appears to be more complicated. One generally expects that as $\kappa L$ increases, end-effects become less significant, and the value of $s_c$ moves toward zero, resulting in a smoothing of the curvature along the chain. However, this is true only for strong screening. Figure 8 represents the dependence of $s_c$ on $\kappa L$ in the strong charging regime, where we observe that $s_c$ has a relatively weak dependence on screening: $s_c$ slowly *increases* as $\kappa L$ is increased and then starts decreasing with further increase in $\kappa L$.

One can understand the appearance of the shoulder region as an end effect. The nonlocal nature of the electrostatic self-interaction leads to enhanced repulsion in

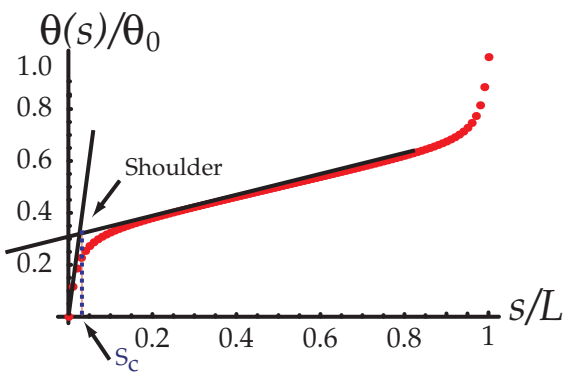


FIG. 6: The position of the shoulder $s_c$ can be obtained as the crossover point of the tangents to the various segments of the profile.

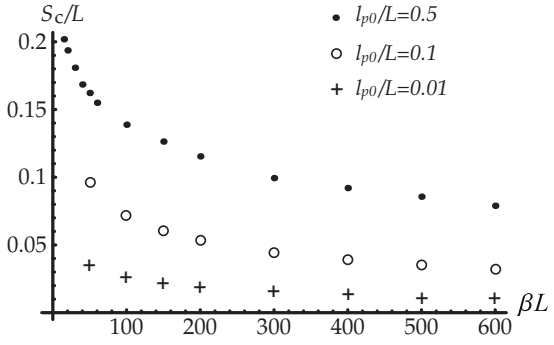


FIG. 7: The position of the shoulder $s_c$ as a function of the charging parameter $\beta L$, for $\kappa L = 0$ and $\ell_{p0}/L$ =0.01 (crosses),0.1 (open circles) and 0.5 (filled circles). As expected, $s_c$ increases as the rod becomes intrinsically more stiff.

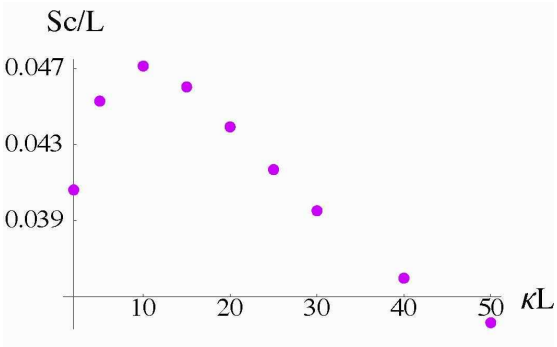


FIG. 8: The position of the shoulder $s_c$ as a function of the screening parameter $\kappa L$, for $\ell_{p0}/L = 0.5$ and $\beta L = 2500$. The re-entrance behavior is characterized by an initial slow increase followed by a relatively faster decay at larger values of the screening parameter.

the interior of the PE as compared to the end-segments. This is mainly due to the fact that there are fewer neighboring pairs at the end-segments to contribute to the mutual repulsion. In other words, one might think of a crossover length scale at the two ends, below which the intrinsic rigidity (that yields a local resistance to bending) dominates the energetics of the chain, while beyond that length scale (i.e. in the interior of the PE) it is the combination of the intrinsic rigidity and the electrostatic repulsion that controls the energetics. Interestingly, such a crossover length scale has been introduced by Barrat and Joanny in their study of the length-scale dependence of the PE rigidity [1, 2]. It is important to note that the Barrat-Joanny crossover length is defined for the crossover in the fluctuations of the angle $\langle\theta(s)^2\rangle$ (that also has a piece-wise linear dependence on $s$). Since the distribution of the angle $\theta(s)$ as controlled by the Hamiltonian in Eq. (7) is Gaussian, both $\langle\theta(s)^2\rangle$ and the energy-minimizing $\theta$ (Eq. 17) are linear functions of $\mathcal{H}(s,s')^{-1}$ (Eq. (8)). Thus we expect that in general the two crossover length scales coincide. Barrat and Joanny propose an expression for the crossover length as

$$s_{c,\mathrm{BJ}} \simeq \sqrt{\frac{\ell_{p0}}{\beta + 4\ell_{p0}\kappa^2}}, \tag{19}$$

which exhibits the limiting forms of $s_{c,\mathrm{BJ}} \sim \sqrt{\ell_{p0}/\beta}$ for $\kappa\sqrt{\ell_{p0}/\beta} \ll 1$, and $s_{c,\mathrm{BJ}} \sim \kappa^{-1}$ for $\kappa\sqrt{\ell_{p0}/\beta} \gg 1$.

The Barrat-Joanny crossover length shows a qualitatively similar behavior to the shoulder position $s_c$ as described above, except for the slow initial increase in Fig. 8 (for $s_c$ as a function of $\kappa$).

There is a way, to reconcile this behavior with the Barrat-Joanny picture. This can be achieved by considering the fact that in their derivation of the expression in Eq. (19) above, they have neglected a logarithmic dependence in the electrostatic nonlocal kernel for technical simplicity. While it is not possible to calculate the correct crossover length in a compact form as in Eq. (19) when the logarithmic factor is taken into account, one can extract the limiting forms of the *augmented* Barrat-Joanny (aBJ) crossover length as

$$s_{c,\mathrm{aBJ}} \sim \begin{cases} \dfrac{1}{\sqrt{\ln\left(\frac{\beta}{\ell_{p0}\kappa^2}\right)}}\sqrt{\ell_{p0}/\beta} & \text{for } \kappa\sqrt{\ell_{p0}/\beta} \ll 1, \\ \kappa^{-1} & \text{for } \kappa\sqrt{\ell_{p0}/\beta} \gg 1, \end{cases} \tag{20}$$

which now exhibits an initial increase in qualitative agreement with Figs. 7 and 8. While this picture can qualitatively account for the aforementioned behaviors, we have not yet been able to achieve a quantitative characterization of the shoulder position $s_c$ as a function of the three dimensionless parameters $\ell_{p0}/L$, $\kappa L$, and $\beta L$, and in particular compare it with the dependencies as suggested by Eq. (20) above, due to the insufficiency of the numerical data.

Having obtained the shape of a charged rod numerically, we can now follow Odijk and calculate the persistence length of PE's.

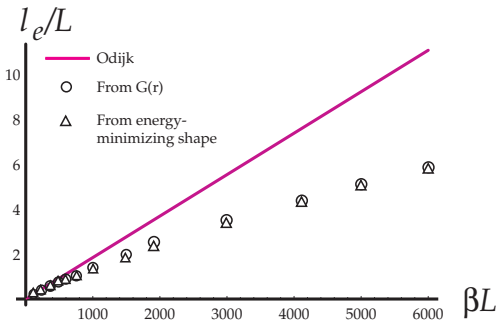


FIG. 9: The electrostatic persistence length, $\ell_e$ obtained by Eq. (22) for $\kappa L = 10$ and $\ell_{p0}/L = 0.5$ at different values of $\beta L$, and comparison with Odijk's persistence length as given by Eq. (6), and the electrostatic persistence length that can be deduced from the radial distribution function of PE's [15, 16].

## V. DERIVATION OF THE PERSISTENCE LENGTH USING ODIJK'S METHOD

There is a straightforward way to calculate the energy of a bent rod, based on the expression for the angle as a function of arc length. The quantity $\theta(s)$ given in Eq. (17) is, to within an additive constant, proportional to $K(s, L) - K(s, 0)$, and the energy of a bent charged rod can be written as

$$\frac{\mathcal{E}}{k_{\rm B}T} = \frac{\theta_0^2}{2}\,\frac{1}{K(0,0) - K(0,L)}. \qquad (21)$$

Details of the calculation leading to Eq. (21) are presented in the Appendix B. According to the definition of the persistence length in terms of the energy of the bent rod, Eq. (1), we have

$$\ell_e = \frac{L}{K(0,0) - K(0,L)} - \ell_{p0}, \qquad (22)$$

where $\ell_e$ is the electrostatic persistence length of the chain as defined in the Sec. II. It is important to note that the kernel $K(s, s')$ depends on the parameters $\beta L$, $\kappa L$, and $\ell_{p0}/L$ through the eigenvalues and eigenfunctions of Eq. (8). Figure 9 shows the values of the electrostatic persistence length, $\ell_e$ obtained by Eq. (22) for $\kappa L = 10$ and $\ell_{p0}/L = 0.5$ at different values of $\beta L$ (triangles). Odijk's persistence length as given by Eq. (6) is also plotted in the figure for comparison (solid line). For small values of $\beta L$, $\ell_e$ coincides with the Odijk persistence length, $\ell_{\rm Odijk}$. As $\beta L$ increases, the deviation of $\ell_e$ and $\ell_{\rm Odijk}$ becomes more significant. The figure also displays the value of the electrostatic persistence length that one can infer from the distribution of end-to-end distances of an ensemble of fluctuating rod-like PE segments (open circles) [15, 16]. There will be more on this subject in the next section.

Our general observation from the comparison of $\ell_e$ with $\ell_{\rm Odijk}$ is that when the two quantities are equal, the bent charged rod is close in shape to an arc of a circle. That is, $\theta(s)$ as a function of $s$ is nearly a straight line as in the case of a neutral chain. This indicates that as charging increases, end-effects become more important and the description of PE's as neutral chains with an adjusted persistence length is inappropriate. It is clear that end-effects play a key role in the elasticity of PE's. Such effects are also apparent in the statistical conformations of the charged rods.

## VI. THE INFLUENCE OF "END-EFFECTS" ON THE STATISTICAL CONFORMATION OF PE'S

The study of the end-to-end radial distribution function, $G(\mathbf{r})$, of a rod-like PE provides an excellent gauge of the statistical conformation of polymers. Using the expression for energy given in Eq. (2), we have obtained values for the quantity

$$G(\mathbf{r}) = \langle \delta(\mathbf{r} - \mathbf{R}) \rangle, \qquad (23)$$

where $\mathbf{R} = \mathbf{r}(L) - \mathbf{r}(0)$. The average in Eq. (23) is over an ensemble of PE chains. The function $G(\mathbf{r})$ is, then the probability that a given chain in the ensemble will have an end-to-end distance equal to $\mathbf{r}$ [15, 16].

With the use of the radial distribution function, we have been able to compare the statistical conformations of PE's with those of uncharged [17] wormlike chains. Figure 10, displays the PE end-to-end distribution (solid line) along with the WLC distribution (dashed line) in a case in which it is not possible to collapse the two distributions on top of each other. The persistence length of the neutral WLC in the figure was adjusted so that the location of the maxima of the two distributions are the same. The plot of the uncharged WLC is for $\ell_p/L = 0.56$. The distribution is for a PE segment with $\ell_{p0}/L = 0.01$, $\kappa L = 1$, and $\beta L = 360$.

Using these parameters, we also calculated the energy-minimizing shape of a PE [Eq. (16)] as shown in the inset of Fig. 10. It is obvious that end effects are not negligible in this case and that the response of the PE to the bending force is different from that of neutral chains. This example indicates a correlation between regimes in which the statistical conformations of a PE chain and that of a WLC differ and circumstances under which the classical, energy-minimizing shape of a PE segment does not trace out the arc of a circle.

There also exist regimes in which the conformational statistics of PE chains in the rod-like limit are identical to those of WLC's with adjusted persistence lengths [22]. For such cases, PE and WLC distributions are indistinguishable to the unaided eye. Figure 11 illustrates an example of this regime. The distribution function of the PE with $\ell_{p0}/L = 0.0001$, $\kappa L = 100$ and $\beta L = 36000$ completely obscures the distribution function of a WLC with the intrinsic persistence length $\ell_p/L = 0.876$. As in the previous example, the energy-minimizing shape of

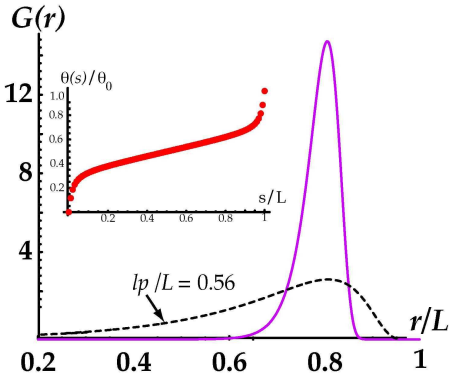


FIG. 10: Comparison of the radial distribution function of a PE (solid line) for $\kappa L = 1$, $\ell_{p0}/L = 0.01$, and $\beta L = 360$, with that of a neutral chain (dashed line). As the inset shows, when the two distributions do not match, the equilibrium configuration of a bent PE is not given by a constant-curvature profile.

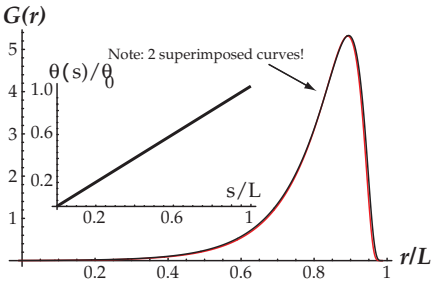


FIG. 11: Comparison of the radial distribution function of a PE for $\kappa L = 100$, $\ell_{p0}/L = 0.0001$, and $\beta L = 36000$, with that of a neutral chain with the intrinsic persistence length $\ell_p/L = 0.876$. The inset shows that when the two distributions collapse on top of each other, the PE bends with constant curvature at equilibrium.

the PE is shown in the inset. It is clear that the energy-minimizing shape of the PE is not distinguishable from that of a neutral chain, as the PE also bends with a constant curvature in this example.

We have found that whenever there is a virtually perfect collapse of the distribution function of a PE onto that of a neutral chain, the persistence length of the neutral chain follows Odijk's prediction, in that, $\ell_p = \ell_e + \ell_{p0}$, where $\ell_p$ is the effective persistence length of the charged chain, and $\ell_e = \ell_{\rm Odijk}$ [11]. It is noteworthy that in these regimes the energy-minimizing shape of PE's is an arc of circle in accordance with the approximation utilized by Odijk in his derivation of Eq. (6).

Figure 9 compares the values of electrostatic persistence length, $\ell_e$ obtained by radial distribution functions (hollow circles) to Odijk's formula (straight solid line). In the figure, the electrostatic persistence length based on Eq. (22) is also plotted (triangles). For small values of $\beta L$, $\ell_e$'s obtained through two different noted methods, coincide with Odijk's persistence length, $\ell_{\rm Odijk}$. As $\beta L$ increases, the deviation of $\ell_e$ from $\ell_{\rm Odijk}$ becomes more significant. However, the electrostatic persistence length obtained through the radial distribution function and the one found by using the "real" shape of the chain match each other quite well.

As we decrease the quantity $\kappa L$, the persistence lengths obtained by distribution function and energy-minimizing shape also start to deviate from each other. This points to the fact that replacing a PE chain with a WLC with an adjusted persistence length is not well-justified in all regimes and that one should use care in the utilization of the notion of an electrostatic persistence length.

## VII. CONCLUSIONS

Our investigation of the equilibrium shape of a bent PE has yielded three striking results. The first is the fact that the Odijk formula, Eq. (6), for the persistence length applies almost perfectly to the case of a fluctuating PE when the bent equilibrium segment has a constant curvature. This is consistent with one of the fundamental assumptions underlying the derivation by Odijk [11].

The second result is a suggestion for an improved calculation of the persistence length based on the energy of the bent PE. This approach appears to yield results in much closer accord with the calculations of the radial distribution function of fluctuating PE segments, even in regimes in which Eq. (6) does not work. We find that the fundamental tactic of extracting a persistence length from the equilibrium energy of a bent PE yields excellent predictions for the effective persistence length of an ensemble of fluctuating PE's over a very wide range of parameters—if, however, one performs a conscientious calculation of the actual shape of the bent PE.

Finally, we are able to characterize the shape of the distorted PE segment in terms of "shoulder" regions, immediately adjacent to the end-points of the chain, at which the curvature is significantly greater than in the chain's interior. It seems highly probable to us that issues of PE energetics are intimately connected to the quantitative features of these shoulder regions. We are not yet able to claim complete resolution of the questions associated with the energetics and conformational statistics of rod-like PE chains. However, the fact that one can, at least in principle, systematically investigate the equilibrium properties of a torqued PE segment gives rise to the expectation of substantial progress in the characterization of the action of the important biomolecules in the family of PE's.

The authors would like to acknowledge helpful discussions with W.M. Gelbart, M. Kardar, R.R. Netz, I. Borukhov, B. Bozorgui, H. Diamant, K. -K. Loh, V. Oganesyan, and G. Zocchi. This research was supported by the National Science Foundation under Grant No. CHE99-88651. One of us (R.G.) would like to thank the group of Prof. de Gennes at Collège de France for its hospitality and support during his visit.

## APPENDIX A: EXPRESSION OF THE ENERGY OF THE BENT PE IN A COSINE BASIS SET

In this Appendix, we outline the method by which one expands the energy of the bent PE in a basis set that automatically satisfies the free boundary conditions at the end of the rod. We begin by expressing the distortion of the rod in terms of the two-dimensional vector $\mathbf{a} = (t_x, t_y)$. This means that

$$\mathbf{t}(s) = \frac{(a_x(s), a_y(s), 1)}{\sqrt{1 + a_x^2(s) + a_y^2(s)}}, \tag{A1}$$

Using the Fourier representation of the screened Coulomb interaction we find

$$\begin{aligned}
\int_0^L ds \int_0^L ds' \frac{e^{-\kappa|\mathbf{r}(s)-\mathbf{r}(s')|}}{|\mathbf{r}(s)-\mathbf{r}(s')|} &= \int \frac{d^3\mathbf{k}}{(2\pi)^3}\frac{4\pi}{k^2+\kappa^2}\int_0^L ds \int_0^L ds' \ \exp\{i\mathbf{k}\cdot[\mathbf{r}(s)-\mathbf{r}(s')]\} \\
&\simeq \int \frac{d^3\mathbf{k}}{(2\pi)^3}\frac{4\pi}{k^2+\kappa^2}\int_0^L ds \int_0^L ds' \ \exp\left\{i\mathbf{k}_\perp\cdot\int_s^{s'} du\ \mathbf{a}(u) - \frac{ik_z}{2}\int_s^{s'} du\ \mathbf{a}(u)^2 + ik_z(s'-s)\right\} \\
&= \int \frac{d^3\mathbf{k}}{(2\pi)^3}\frac{4\pi}{k^2+\kappa^2}\int_0^L ds \int_0^L ds' \ e^{ik_z(s'-s)} \\
&\quad \times \left[1 - \frac{1}{2}\left(\mathbf{k}_\perp\cdot\int_s^{s'} du\ \mathbf{a}(u)\right)^2 - \frac{ik_z}{2}\int_s^{s'} du\ \mathbf{a}(u)^2 + O(a^3)\right].
\end{aligned} \tag{A2}$$

The quantity $\mathbf{k}_\perp$ is the projection of the wave vector $\mathbf{k}$ on the $x$-$y$ plane. The quantity $k_z$ is the $z$-component of that three-dimensional vector. Next, we use the series expansion $\mathbf{a}(s) = \sqrt{2}\sum_{n=0}^{\infty}\mathbf{A}_n\cos\left(\frac{n\pi s}{L}\right)$ as appropriate for the open-end boundary condition, and assume for simplicity that $\mathbf{r}$ is, on average, oriented along the $z$-axis so that $\mathbf{A}_0 = \frac{1}{\sqrt{2}}\int_0^L ds\ \mathbf{a}(s) = 0$. This leads to the following representation of the Hamiltonian of the PE rod

$$\frac{\mathcal{E}}{k_{\rm B}T} = \frac{\ell_{p0}}{2L}\sum_{n=1}^{\infty}(n\pi)^2 A_n^2 + \frac{\beta L}{2}\sum_{n,m=1}^{\infty}\mathbf{A}_n\cdot\mathbf{A}_m E_{nm}, \tag{A3}$$

where

$$\begin{aligned}
E_{nm} &= \frac{4L}{\pi nm}\int_{-\infty}^{\infty}\frac{dk_z}{2\pi}\left(k_z^2+\kappa^2\right)\ln\left[\frac{(\pi/d)^2+\kappa^2+k_z^2}{\kappa^2+k_z^2}\right] \\
&\times \left\{\cos\left[\frac{\pi}{2}(n-m)\right]\left[\frac{\sin\left(\frac{k_zL}{2}\right)\sin\left(\frac{k_zL}{2}-\frac{\pi(n-m)}{2}\right)}{k_z\left[k_z-(n-m)\pi/L\right]} - \frac{\sin\left(\frac{k_zL}{2}-\frac{\pi n}{2}\right)\sin\left(\frac{k_zL}{2}-\frac{\pi m}{2}\right)}{(k_z-n\pi/L)(k_z-m\pi/L)}\right]\right. \\
&\left. -\cos\left[\frac{\pi}{2}(n+m)\right]\left[\frac{\sin\left(\frac{k_zL}{2}\right)\sin\left(\frac{k_zL}{2}-\frac{\pi(n+m)}{2}\right)}{k_z[k_z-(n+m)\pi/L]} - \frac{\sin\left(\frac{k_zL}{2}+\frac{\pi n}{2}\right)\sin\left(\frac{k_zL}{2}-\frac{\pi m}{2}\right)}{(k_z+n\pi/L)(k_z-m\pi/L)}\right]\right\},
\end{aligned} \tag{A4}$$

are the elements of the electrostatic energy matrix in the cosine basis set. It is now sufficient to replace $a_x(s)$ by $\theta_x(s)$, and similarly for $a_y(s)$.

A thorough investigation of the energy matrix (Eq. (A3)) is given in Refs. [15, 16]. The requirement that the coarse graining length $b$ not exceed the smallest wavelengths appearing in the cosine basis set puts a restriction on the size of the matrix energy. If the length of the PE is $L$, this means that the size, $N$, of the basis set satisfies $N \le L/b$. At no point in our calculations was this inequality violated.

An advantage of the cosine basis set, quite aside from automatic satisfaction of the open boundary conditions, is that when $n$ and $m$ are large, the matrix elements in Eq. (A3) are dominated by those for which $m = n$. This reflects the dominance of elastic energy at short wave-

lengths.

## APPENDIX B: CALCULATION OF THE MINIMUM ENERGY OF A BENT ROD

In this Appendix, the minimum energy of a charged chain that is slightly deformed about the rodlike configuration with the use of Eq. (18) is derived. We begin with the expression for the angle when the ends of the rod have been torqued:

$$\theta(s) \propto K(s,0) - K(s,L). \tag{B1}$$

Here the total arclength of the rod is assumed to be $L$. The relationship between the kernel $K(s,s')$ as given by Eq. (18) and the energy operator $\mathcal{H}(s,s')$ as given by Eq. (8) is

$$\int_0^L ds''\ \mathcal{H}(s,s'')K(s'',s) = \delta(s-s'). \tag{B2}$$

To obtain the proportionality constant in Eq. (B1), let us assume that the angle at $s = 0$ is $-\theta_0/2$, while the angle at $s = L$ is $\theta_0/2$. Then, we have

$$\theta(s) = \frac{\theta_0}{2}\ \frac{K(s,0) - K(s,L)}{K(0,L) - K(0,0)}. \tag{B3}$$

The above kernel is symmetric, in that $K(x,y) = K(y,x)$; furthermore, there is reflection symmetry in the looped rod in that $K(0,0) = K(L,L)$. The next step is to note that the energy of the rod is the expectation value of the energy operator, i.e.

$$\frac{\mathcal{E}}{k_{\rm B}T} = \frac{1}{2}\int_0^L \int_0^L dsds'\ \theta(s)\mathcal{H}(s,s')\theta(s'). \tag{B4}$$

If we plug in the solution (B3) for $\theta(s)$ in Eq. (7) and make use of the relation (B2), we end up with the expression in Eq. (21) for the energy of the bent rod.


[1] J.-L. Barratt and J.-L. Joanny, Europhysics Letters **24**, 333 (1993).

[2] J.-L. Barratt and J.-L. Joanny, Adv. Chem. Phys. **XCIV**, 1 (1996).

[3] B. Y. Ha and D. Thirumalai, Journal of Chemical Physics **110**, 7533 (1999).

[4] M. J. Stevens and K. Kremer, Journal of Chemical Physics **103**, 1669 (1995).

[5] G. Ariel and D. Andelman, cond-mat/0206361.

[6] R. R. Netz and H. Orland, European Physical Journal B **8**, 81 (1999).

[7] L. Eichinger, B. Koppel, A. A. Noegel, M. Schleicher, M. Schliwa, K. Weijer, W. Witke, and P. A. Janmey, Biophys J **70**, 1054 (1996).

[8] P. A. Janmey, Curr. Op. Cell. Biol. **2**, 4 (1999).

[9] E. Helfer, S. Harlepp, L. Bourdieu, J. Robert, F. C. MacKintosh, and D. Chatenay, Physical Review Letters **85**, 457 (2000).

[10] L. D. Landau, L. P. Pitaevskii, and E. M. Lifshits, *Statistical physics*, Pergamon international library of science, technology, engineering, and social studies (Pergamon Press, Oxford ; New York, 1980), 3rd ed.

[11] T. Odijk, J. Polym. Sci. **15**, 477 (1977).

[12] J. Skolnick and M. Fixman, Macromolecules **10**, 944 (1977).

[13] A. R. Khokhlov and K. A. Khachaturian, Polymer **23**, 1742 (1982).

[14] T. Witten and H. Li, Macromolecules **28**, 5921 (1995).

[15] R. Zandi, J. Rudnick, and R. Golestanian, European Physical Journal E **9**, 41 (2002).

[16] R. Zandi, J. Rudnick, and R. Golestanian, Physical Review E (Statistical Physics, Plasmas, Fluids, and Related Interdisciplinary Topics) **67**, 021803 (2003).

[17] J. Wilhelm and E. Frey, Physical Review Letters **77**, 2581 (1996).

[18] O. Kratky and G. Porod, Recl. Trav. Chim. **68**, 1106 (1949).

[19] Numerical evaluation of $G(r)$ based on a Monte-Carlo simulation in Ref. [17] reveals that the approximation taken for analytical calculation of $G(r)$ is good when $L/\ell_p \leq 2$. Thus we restrict our attention to this regime and assume that $\ell_{p0}/L = 0.5$ is the onset of rodlike limit.

[20] R. Golestanian, M. Kardar, and T. B. Liverpool, Physical Review Letters **82**, 4456 (1999).

[21] R. Golestanian and T. B. Liverpool, Physical Review E. **66**, 51802 (2002).

[22] In Refs. [15, 16], we have identified the regimes in which the conformational statistcs of a PE differ from those of a WLC and those in which the PE behaves like a WLC.